Vol. 23, No. 1(2024) IA24161
Revista Mexicana de Ingeniería Química

Biosorption performance evaluation of azo dyes Reactive Red 2 and Reactive Blue 4 on thermally sterilized biomass of *Cladosporium tenuissimum* fungus

Evaluación en el desempeño de la biosorción de los colorantes azo Reactivo Rojo 2 y Reactivo Azul 4 en la biomasa térmicamente esterilizada del hongo *Cladosporium tenuissimum*

A. Jiménez-González[1], E. N. Tec-Caamal[2], S.A. Medina-Moreno[1]*
[1]*Departamento de Biotecnología, Universidad Politécnica de Pachuca. Ex-Hacienda de Santa Bárbara, Mpio. Zempoala, Hgo., C.P. 43830, Carr. Pachuca Cd. Sahagún Km. 20.*
[2]*Centre of Bioengineering, School of Engineering and Sciences, Tecnologico de Monterrey, Campus Querétaro, Av. Epigmenio González 500, Querétaro 76130, México.*
Received: September 25, 2023; Accepted: January 13, 2024

Abstract
The present study evaluated the performance in the biosorption of the azo dyes reactive red 2 (RDR2) and reactive blue 4 (RDB4) on thermally sterilized biomass of the fungus *Cladosporium tenuissimum*. A decrease in the initial pH and an increase in the temperature improved the biosorption, reaching the higher removal efficiencies of RDR2 (98.5%) and RDB4 (94.1%) at pH 3 and 40 °C. A pseudo-second-order model explained the biosorption kinetics of RDR2 and RDB4. The intraparticle diffusion model showed that the biosorption process was controlled initially by diffusion rate and, later, by the biomass surface saturation with the dye molecules. The Langmuir isotherm explained well the biosorption equilibrium, achieving the maximum biomass biosorption capacities ($q_{\max}$) of 76.67 mg g^{-1} for RDR2 and 70.60 mg g^{-1} for RDB4 at pH 3 and 40 ºC. According to the dimensionless separation factor (R_L) values and the thermodynamic evaluation, the biosorption process was favorable, reversible, spontaneous, and endothermic. FTIR analysis of unloaded and loaded biomass with the dyes confirmed the interactions between dye molecules and functional groups on the fungal biomass surface. The thermally sterilized biomass of *Cladosporium tenuissimum* can be used as a biosorbent biomaterial for bioprocess design in removing the azo dyes active red 2 and reactive blue 4 from textile wastewater.
Keywords: Biosorption, fungal biomass, azo dyes, kinetics, isotherms.

Resumen
El presente estudio evaluó el desempeño en la biosorción de los colorantes azoicos rojo reactivo 2 (RDR2) y azul reactivo 4 (RDB4) sobre biomasa térmicamente esterilizada del hongo *Cladosporium tenuissimum*. Una disminución del pH inicial y un aumento de la temperatura mejoraron la biosorción, alcanzando mayores eficiencias de eliminación de RDR2 (98,5%) y RDB4 (94,1%) a pH 3 y 40 °C. Un modelo de pseudo-segundo-orden explicó la cinética de biosorción de RDR2 y RDB4. El modelo de difusión intrapartícula mostró que el proceso de biosorción estaba controlado inicialmente por la velocidad de difusión y, posteriormente, por la saturación de la superficie de la biomasa con las moléculas de colorante. La isoterma de Langmuir explicó bien el equilibrio de biosorción, logrando capacidades máximas de biosorción de la biomasa ($q_{\max}$) de 76,67 mg g^{-1} para RDR2 y 70,60 mg g^{-1} para RDB4 a pH 3 y 40 ºC. Según los valores del factor de separación adimensional (R_L) y la evaluación termodinámica, el proceso de biosorción fue favorable, reversible, espontáneo y endotérmico. El análisis FTIR de biomasa cargada y descargada con los colorantes confirmó las interacciones entre las moléculas de colorante y los grupos funcionales en la superficie de la biomasa fúngica. La biomasa esterilizada térmicamente de *Cladosporium tenuissimum* puede ser utilizada como biomaterial biosorbente para el diseño de bioprocesos para eliminar los colorantes azoicos rojo activo 2 y azul reactivo 4 de aguas residuales textiles.
Palabras clave: Biosorción, biomasa fúngica, colorantes azo, cinética, isotermas.

*Corresponding author. *E-mail*: samm67@upp.edu.mx;
https://doi.org/10.24275/rmiq/IA24161
ISSN:1665-2738, *issn-e*: 2395-8472

1 Introduction

The textile, cosmetic, pharmaceutical, and paper industries currently utilize over 10,000 distinct types of synthetic dyes, with global production estimated to range from 7×10^5 to 1×10^6 tons per year (Rangabhashiyam *et al*., 2018). Within the manufacturing processes of these industries, around 10% to 15% of the dyes are discharged or lost in the effluents (Al-Amrani *et al*., 2014), with the textile industry being a significant contributor to synthetic dye discharges with a high water consume (Singh and Khajuria, 2018; Gonzales-Condori *et al*., 2023). The release of dyes into aquatic ecosystems not only negatively impacts the visual environment but also inflicts harm upon aquatic organisms by obstructing light necessary for photosynthesis and depleting dissolved oxygen concentration (Saratale *et al*., 2011). Furthermore, due to their chemical structure, dyes exhibit high toxicity and carcinogenic potential to living organisms and humans (Liao *et al*., 2013). Reactive azo dyes, which prominently find use in the textile industry, comprise around 60% to 70% and are characterized by containing one or more chromophore azo groups (-N=N-) along with reactive functional groups such as chlorotriazine, vinyl sulfone, and trichloropyrimidine (Danouche *et al*., 2021).

Several physicochemical methods such as precipitation, photo-oxidation, coagulation, flocculation, chemical reduction, adsorption, electrochemical treatment, and membrane processes have been used to remove reactive azo dyes from wastewater (Arslan *et al*., 2016). However, these methods require high energy levels, are expensive because of the devices and materials employed, and can generate more toxic byproducts than reactive azo dyes (He *et al*., 2016). On the other hand, biological methods based on microorganisms represent one alternative for treating wastewater polluted with reactive azo dyes because they are relatively low-cost and eco-friendly to the environment (Kumar *et al*., 2014). Within microorganisms used, the fungi can remove reactive azo dyes from aquatic polluted systems by two mechanisms: enzymatic biodegradation and biosorption (Medina-Moreno *et al*., 2012). Nevertheless, owing to the structural stability and complexity of the reactive azo dyes, enzymatic biodegradation by fungi is usually partial, eliminating the coloration in the wastewater but leading to the formation of byproducts (Dionel *et al*., 2019). Fungal biomass used for the biosorption process of reactive azo dyes is feasible since biomass as a biosorbent is economical and relatively easy to propagate by fermentation techniques (Aksu and Karabayir, 2008). The fungal biomass biosorption capability of the reactive azo dyes is due to cell wall characteristics, whose composition on biomolecules such as polysaccharides, lipoproteins, and lipopolysaccharides are responsible for binding pollutant molecules because they have functional organic groups such as carboxyl, amino, thiol, sulfhydryl, and phosphate (Akar *et al*., 2009a).

The biosorption capability of fungal biomass inactivated (dead cells) by sterilization has shown to be higher than that of fungal biomass active (cell live), which has been observed for different fungi, such as *Panus tigrinus*, *Diaporthe schini*, and *Sarocladium sp* ADH17 with the dyes reactive blue 19, crystal violet, and remazol black, respectively (Mustafa *et al*., 2017; Grassi *et al*., 2019; Nouri *et al*., 2021). The improvement in the biosorption of dyes by inactive biomass has been attributed to the further exposure of available functional groups as sorption sites on the cell surface (Azin and Moghimi, 2018). On the other hand, there are extensive reports about the biomass efficiency of the genus fungi *Cladosporium sp* on the biosorption of metals (Garza-González *et al*., 2017; Ahluwalia and Goyal, 2010; Legorreta-Castañeda *et al*., 2022) and other hazardous compounds (Juhasz *et al*., 2002; Juhasz *et al*., 2003; Dave and Dikshit, 2014). However, to our knowledge, information on the use of *Cladosporium sp* biomass in the biosorption of dyes is scarce with respect to the diversity of chemical dyes. The present study aimed to evaluate the biosorption performance of azo dyes Reactive Red 2 (RDR2) and Reactive Blue 4 (RDB4) onto thermally sterilized biomass of the fungus *Cladosporium tenuissimum*. RDR2 and RDB4 are two of the azo dyes most commonly used in the textile industry and, hence, two of the main pollutant dyes in wastewater (Axelsson *et al*., 2006). In the study, diverse experimental assays with the sterilized biomass of *C. tenuissimum* were conducted to evaluate the biosorbent dosage, pH, and temperature effects on the biosorption removal efficiency of both dyes. Moreover, the process was characterized by determining kinetics, equilibrium, and thermodynamic parameters by fitting the experimental data to diverse biosorption models and conducting an FTIR analysis.

2 Material and methods

2.1 Azo dyes

The azo dyes Reactive Red 2 (RDR2, Disodium (3Z)-5-[(4,6-dichloro-1,3,5-triazin-2-yl) amino]-4-oxo-3- (phenylhydrazono)-3,4-dihydro-2,7-naphthalenedisulfonate) with molecular weight 615.13 g mol^{-1}, and azo dye Reactive Blue 4 (RDB4, 1-Amino-4- [3-(4, 6-dichlorotriazin-2-ylamino)-4-sulfophenylamino] anthraquinone-2-sulfonic acid) with molecular

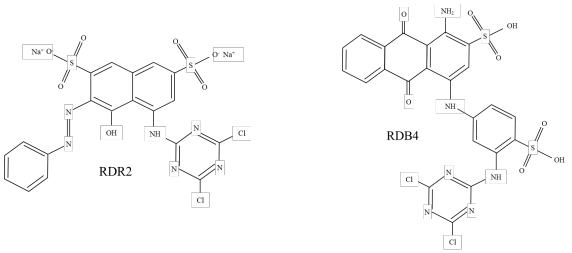

Figure 1. Structures of azo dye Reactive Red 2 (RDR2; Disodium (3Z)-5-[(4,6-dichloro-1,3,5-triazin-2-yl) amino]-4-oxo-3- (phenylhydrazono)-3,4-dihydro-2,7-naphthalenedisulfonate) and azo dye Reactive Blue 4 (RDB4; 1-Amino-4- [3-(4, 6-dichlorotriazin-2-ylamino)-4-sulfophenylamino] anthraquinone-2-sulfonic acid).

weight 637.4 g mol^{-1}, were acquired from Sigma Aldrich. The structures of the azo dyes are shown in Figure 1. Solutions of 300 mg L^{-1} of each azo dye were prepared in distilled water and stocked for use in the experimental assays. The maximum absorbance of the solutions of RDR2 and RDB4 were in the wavelengths (λ_{max}) of 575 and 592 nm, respectively, determined with a UV-visible spectrophotometer (AquaMate).

2.2 *Cladosporium tenuissimum fungus*

The fungus was isolated from Mineral del Monte's bovine cattle slaughterhouse wastewater (Hidalgo, Mexico) by Robles-Morales *et al.* (2021), assigning it the identifier code ACT2. Fungus was maintained by continuous subcultures in Petri dishes with potato dextrose agar (PDA) incubated at 32°C and stocked at 4 ºC. The extraction and amplification by PCR of the fungus DNA was conducted in the Genomic Biotechnology Center of the National Polytechnic Institute (CBG-IPN). The fungus was identified via ribosomal DNA sequencing, considering the regions ITS1-5.8S-ITS2 and D1/D2 of the subunit 28S (LSU). Sequence comparison and alignment were conducted with the Basic Local Alignment Search Tool (BLAST) of the National Center for Biotechnology Information (NCBI) database, using the Clustal X program (Thompson *et al.*, 1997). BEAST v1.8.0 program (Drummond *et al.*, 2002) was employed, using the Bayesian algorithm through amino acids substitution model by the method of maximum likelihood WAG (Whelan and Goldman 2001). Phylogenetic analysis was conducted using the Markov Chain Monte Carlo algorithm (MCMC), which ran ten million generations. The Tree Annotator v1.7.4 program was used for the tree consensus with the predetermined parameters. The program Fig Tree v1.4, edited with the iTOL program, was used for the graphical view of the generated phylogenetic tree. The sequence comparison and alignment with the known available

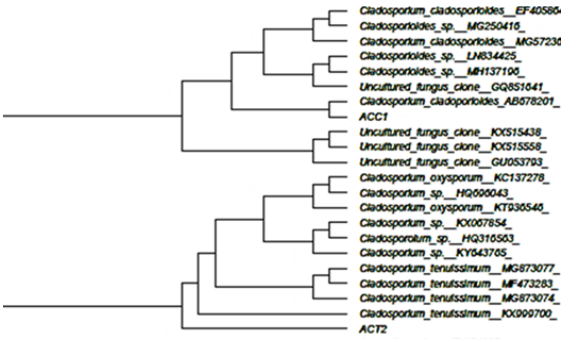

Fig. 2 Phylogenetic tree of maximum similarity for the isolated strain ACT2 with the fungus *Cladosporium tenuissimum*.

at GenBank shared more than 98% similarities with *Cladosporium tenuissimum* (Figure 2).

2.3 *Cladosporium tenuissimum biomass preparation as biosorbent*

The fungal biomass was propagated in several 5 L batches of liquid culture medium in an agitated tank bioreactor using the applikon *ez*-control system. The mineral composition of the culture medium (g L^{-1}) was KH_2PO_4 (2), K_2HPO_4 (2.4), $MgSO_4$ (0.3), $FeSO_4$ (0.015), $ZnSO_4$ (0.015), $CuSO_4$ (0.01), and $MnSO_4$ (0.01). Sacharosse $C_{12}H_{22}O_{11}$ (20 gL^{-1}) was used as a carbon and energy source, and ammonium nitrate NH_4NO_3 (6.5 gL^{-1}) was used as a nitrogen source in a C/N ratio of 4.2 to promote fungal biomass growth. Each batch had a duration of 72 h, and the culture conditions in the bioreactor were pH 7 (buffered with phosphate salts), 27 °C, and an impeller velocity of 120 rpm. At the end of the cultures, the medium with the biomass was sterilized at 121 ºC for 30 min; posteriorly, inactive biomass was harvested, filtered under vacuum on Whatman No. 42 filter paper, and dried at 60 ºC for 12 hours. Dry biomass was powdered with an electric mill for grains and stocked in a desiccator for its posterior use. It was assumed that fungal biomass produced in controlled conditions and their posterior standardized treatment allows obtaining a biosorbent material with a biosorption capability that can be maintained through subsequent batches.

2.4 *Biosorption assays*

In all the biosorption assays conducted with the dyes RBD2, RDB4, and *C. tenuissimum* biomass, 50 mL Erlenmeyer flasks with baffles and 20 mL of the dye solution at 300 mg L^{-1} and initial pH adjusted were used as experimental units. To evaluate the effect of the biosorbent dosage on dye removal, the initial pH of the dye solution was adjusted to 5 with HCl 0.5 M, and biomass was added at dosages of 1-7 g L^{-1}. The experimental units were run in triplicate and kept

at 30 °C and 120 rpm in a rotatory shaker for 5 h. To evaluate the effects of pH and temperature on dye removal, the initial pH values used in the dye solutions were 3, 5, and 7, adjusted with HCl and NaOH 0.5 M, at temperatures of 20, 30, and 40 ºC, respectively, with a biomass dosage of 5 g L^{-1}. The experimental units were run in triplicate at 120 rpm for 5 h. To evaluate the contact time and determine the biosorption kinetics parameters at several temperatures, the initial pH of the dye solution was adjusted to 5, using a biomass dosage of 5 g L^{-1} and sampling at different times between 5 and 130 min. The experimental units were run in triplicate at 120 rpm and 20, 30, and 40 ºC. In the biosorption isotherms construction, the biomass dosage used was 1-5 g L^{-1} with initial pH values of 3, 5, and 7 at 20, 30, and 40 ºC. The experimental units were run in triplicates at 120 rpm and for 10 h to ensure they reached the equilibrium. At the end of all biosorption assays, the volume of the experimental units was centrifuged at 3,000 g. The dye concentration in the equilibrium was determined from supernatant spectrophotometrically (UV-visible spectrophotometer, AquaMate) at the maximum absorbance wavelength of RDR2 and RDB4. Figure 3 shows a scheme of the strategy conducted in the biosorption assays. The dye removal efficiency by biosorption (%) and experimental biomass biosorption capacity q_{exp} (mg g^{-1}) were estimated by:

$$\text{Removal}\ (\%) = \left(\frac{C_0 - C_e}{C_0}\right) \times 100 \tag{1}$$

$$q_{exp} = \frac{C_0 - C_e}{D_B} \tag{2}$$

Where C_0 and C_e are the initial and equilibrium dye concentrations (mg L^{-1}), respectively, and D_B is the biomass or biosorbent dosage (g L^{-1}). To elucidate the functional groups involved in the biosorption of RDR2 and RDB4, the sterilized and dry fungus biomass without dye and loaded with dyes due to biosorption was analyzed by Fourier Transform Infrared Spectroscopy (FTIR) with Thermo scientific Nicolet 6700 FT-IR spectrometer in the spectral range of 4000 to 500 cm^{-1}.

2.5 *Biosorption kinetics*

To evaluate kinetically and characterize the dyes biosorption of RDR2 and RDB4 on sterilized biomass of *C. tenuissimum* by mean of the determination of the parameters, the experimental data of the biosorption capacity were fitted at the kinetic models of pseudo-first-order, pseudo-second-order, and intraparticle diffusion with the R^2 coefficient as the fit criterion. The linearized form of the pseudo-first-order model is (Lagergren, 1898):

$$\ln(q_e - q_t) = \ln q_e - k_1 \cdot t \tag{3}$$

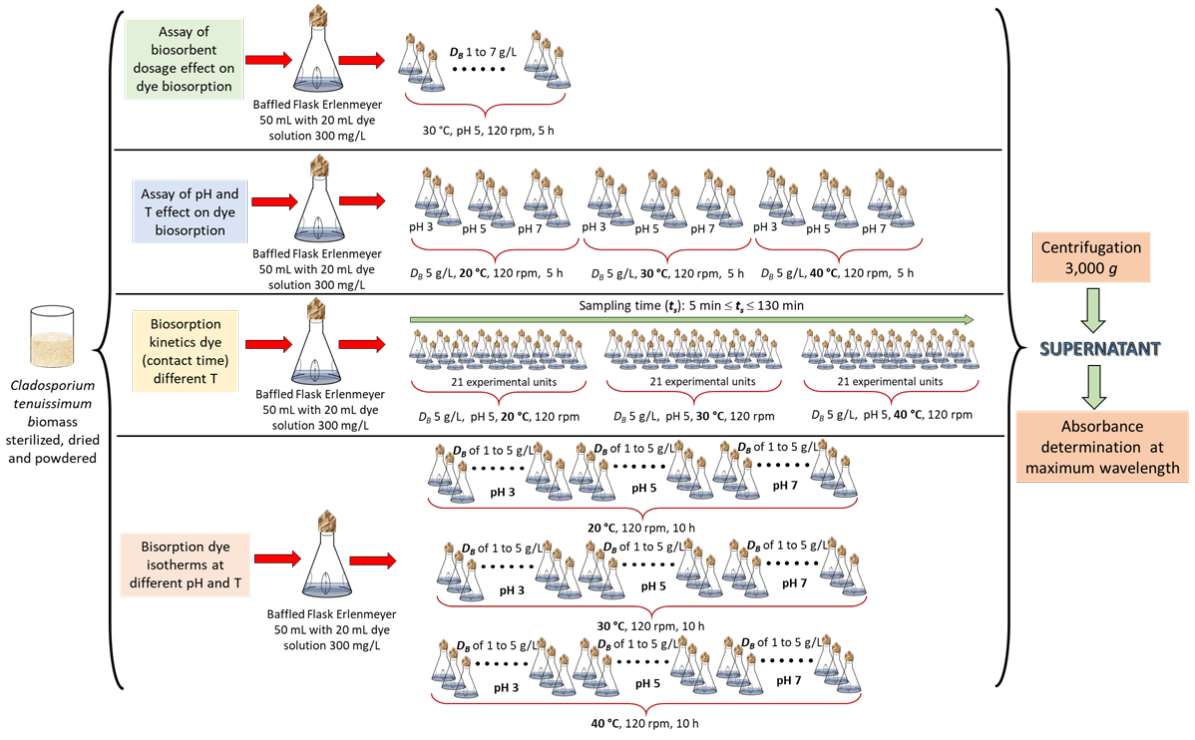

Figure 3. Strategy conducted in the biosorption assays of the dyes RDR2 and RDB4 on thermally inactive *Cladosporium tenuissimum* biomass.

The linearized form of the pseudo-second-order model is (Ho and Mckay, 1998):

$$\frac{t}{q_t} = \frac{1}{k_2 \cdot q_e^2} + \frac{1}{q_e} t \tag{4}$$

The intraparticle diffusion model is (Weber and Morris, 1963):

$$q_t = k_D \cdot t^{0.5} + B \tag{5}$$

Where q_e is the biosorption at the equilibrium (mg g^{-1}), q_t the biosorption at any time (mg g^{-1}), k_1 is the rate first order constant (min^{-1}), k_2 is the rate equilibrium second order constant (g mg^{-1} min^{-1}), k_D is the intraparticle diffusion rate constant (mg g^{-1} $min^{-1/2}$) and B is a constant related to the thickness of the biosorbent boundary layer (mg g^{-1} $min^{-1/2}$).

2.6 *Biosorption isotherms*

The biosorption equilibrium of RDR2 and RDB4 on *C. tenuissimum* sterilized biomass was characterized by fitting the experimental data to the isotherms of Langmuir, Temkin, and Dubinin-Radushkevich. The Langmuir isotherm is given by:

$$q_e = \frac{q_{\max} \cdot C_e \cdot K_L}{1 + C_e \cdot K_L} \tag{6}$$

$q_{\max}$ is the maximum biosorption capacity (mg g^{-1}) and K_L is the Langmuir constant (L mg^{-1}). The linearized equation of Langmuir is:

$$\frac{C_e}{q_e} = \frac{1}{q_{\max} \cdot K_L} + \frac{C_e}{q_{\max}} \tag{7}$$

In additionally to $q_{\max}$ and K_L, another critical parameter from the Langmuir isotherm is the dimensionless separation factor (R_L), defined as follows (Abdel-Aty *et al*. 2015):

$$R_L = \frac{1}{1 + K_L \cdot C_0} \tag{8}$$

The R_L values indicate whether the biosorption process is irreversible ($R_L = 0$), favorable and reversible ($0 < R_L < 1$), linear ($R_L = 1$), or not favorable ($R_L > 1$). The linearized form of Temkin isotherm is:

$$\ln q_e = \frac{RT}{b_T} \ln C_e + \frac{RT}{b_T} \ln K_T \tag{9}$$

R is the universal gas constant (8.314 J mol^{-1} K^{-1}), T is absolute temperature (K), b_T is a Temkin constant which is related to the heat of adsorption (J mol^{-1}), and K_T is equilibrium binding energy (L g^{-1}). The Dubinin-Radushkevich isotherm is:

$$\ln q_e = \ln q_{DR} - K_{DR} \cdot \varepsilon^2 \tag{10}$$

Where:

$$\varepsilon = RT \ln\left(\frac{C_e + 1}{C_e}\right) \tag{11}$$

q_{DR} is the maximum biosorption capability (mg g^{-1}) and K_{DR} is the Dubinin-Radushkevich constant (mol^2 J^{-2}). From K_{DR} the binding free energy (E, J mol^{-1}) between sorbate (dyes) and biosorbent (biomass) is determined by:

$$E = \frac{1}{\sqrt{2K_{DR}}} \tag{12}$$

If E values are lesser than 8 kJ mol^{-1}, the biosorption is of type physical. While for E values between 8 and 16 kJ mol^{-1}, the biosorption is of type chemical (Saleh, 2022). In the experimental data fit to the different isotherms models, in addition to the R^2 coefficient, the Root Mean Squared Error (RMSE) was also used as a criterion.

$$RMSE(q_e) = \sqrt{\frac{1}{n-1} \cdot \sum_{i=1}^{n} \left(q_e - q_e^{exp}\right)^2} \tag{13}$$

2.7 *Bisorption thermodynamics*

Thermodynamic parameters of the biosorption of RDR2 and RDB4 on sterilized *C. tenuissimum* biomass were estimated by (Liu, 2009):

$$\Delta G^0 = -RT \ln K_L \tag{14}$$

$$\Delta G^0 = \Delta H^0 - T\Delta S^0 \tag{15}$$

Equaling equations (14) and (15):

$$\ln K_L = -\frac{\Delta H^0}{R} \cdot \frac{1}{T} + \frac{\Delta S^0}{R} \tag{16}$$

Standards free energy, enthalpy, and entropy were estimated from equations (14) and (16), where K_L the Langmuir constant was expressed in L mol^{-1}.

3 Results and discussion

3.1 *Effect of the biomass dosage as biosorbent*

The effect of biomass dosage on the removal efficiency by biosorption of RDR2 and RDB4 with a C_0 of 300 mg L^{-1}, 30 ºC, and pH 5 are shown in Figures 4a and 4b, respectively. For RDR2, a dosage of 0.95 g L^{-1} reached a removal efficiency by biosorption of 50%, increasing to values upper to 96.5% for biomass dosage from 5 g L^{-1}. Referring to RDB4, a removal efficiency by biosorption of 50% was achieved with a dosage of 1.1 g L^{-1}, and for dosages, upper at the 5 g L^{-1} was higher to 92.8%. The available surface for biosorption explains the increase in the

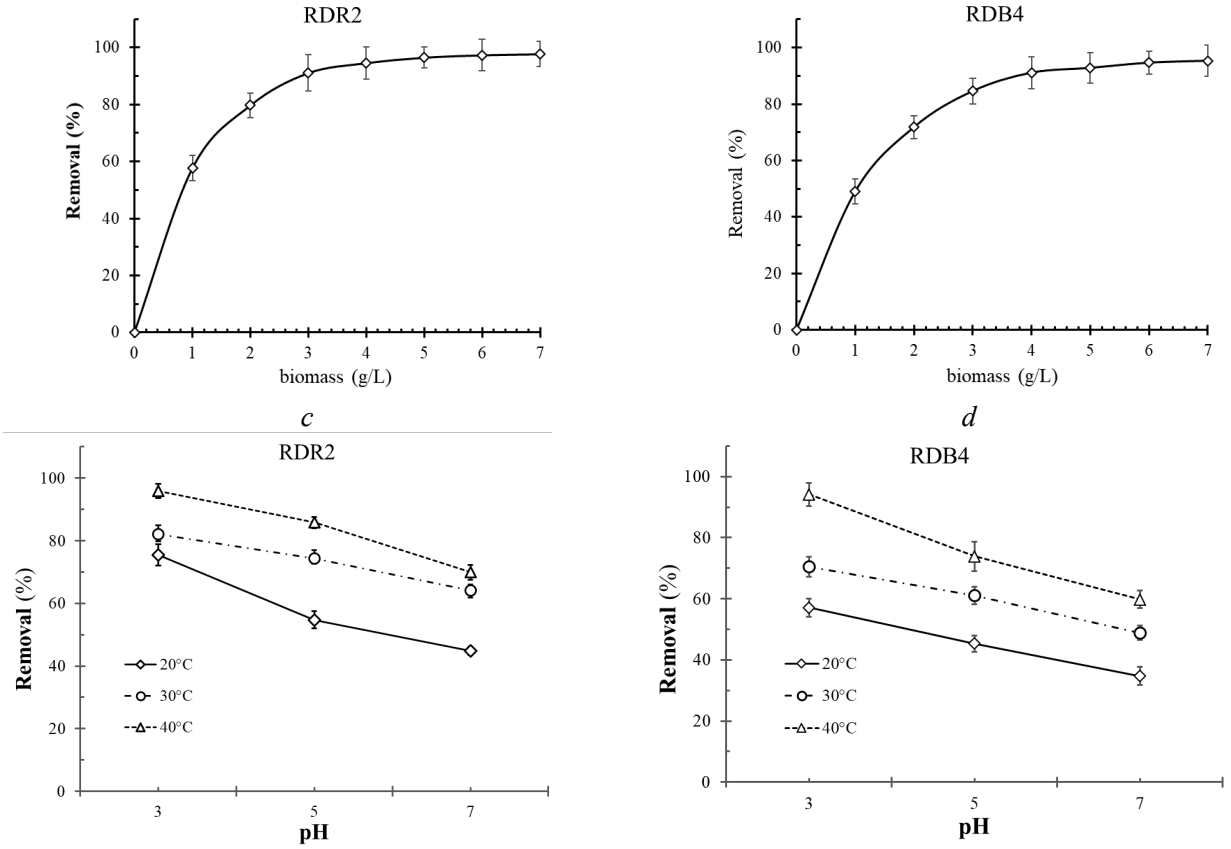

Figure 4. Effects of the biomass dosage (300 mg L^{-1} dyes, 30 ºC and pH 5) in the removal efficiency by biosorption of RDR2 (a) and RDB4 (b). Effects of the initial pH (3, 5, 7) and temperature (20, 30 and 40ºC) at biomass dosage of 5 g L^{-1} on the removal efficiency by biosorption of RDR2 (c) and RDB4 (d).

removal biosorption efficiency because of the higher number of active sites to bind dye molecules. The later constant trend in the removal efficiency by biosorption may be attributed to the saturation of the active sites available on the biomass surface. It is interesting to note that the removal efficiency by biosorption in the case of RDR2 is slightly higher than that of RDB4, which may be due to differences in the molecule structure sizes (molecular weight of RDR2 is 614.13 g mol^{-1} against 637.4 g mol^{-1} of the RDB4). The RDR2 molecule size is slightly smaller than the RDB4 molecule. Therefore, a greater number of molecules can interact with the biomass surface, reflecting a higher removal efficiency by biosorption. Similar results in the removal efficiency by biosorption have been observed for RDR2 and RDB4 with other fungi. With the champignon fungus *Agaricus bisporus*, using a biomass dosage of 2.5 g L^{-1} and a RDR2 concentration of 100 mg L^{-1}, a removal efficiency higher than 93.5% was achieved (Akar and Divriklioglu, 2010). With the fungus *Rhizopus oryzae* biomass, a saturation with a removal efficiency of 98.0% was achieved with a dosage of 8 g L^{-1} and a dye concentration of 100 mg L^{-1} (Bagchi *et al*., 2021).

3.2 Effect of pH and temperature

The pH and temperature are two factors that strongly affect the biosorption process (Dávila-Parra *et al*., 2022). The combined effect of both was investigated in the biosorption of RDR2 and RDB4 onto sterilized biomass of *C. tenuissimum*. The pH initial values used were 3, 5, and 7, while for temperature were 20, 30, and 40 ºC. Figures 4c and 4d show the combined effect of pH initial and temperature on the removal efficiency by biosorption of the RDR2 and RDB4, respectively. For the three temperatures, increases in the pH initial of the medium lead to a decrease in the removal efficiency by biosorption for both dyes. In contrast, for the three pH, increases in the temperature lead to an increase in the removal efficiency by biosorption. In the RDR2 case, the higher removal efficiency by biosorption was 95.8% at pH 3 and 40 ºC, and the lower was 44.8% at pH 7 and 20 ºC. For RDB4, the higher removal efficiency by biosorption was 94.1% at pH 3 and 40 ºC, and the lower 34.7% at pH 7 and 20 ºC. The same effect of the pH and temperature has been observed on the biosorption of diverse anionic dyes with the biomass of other fungi, as are the azo dye Reactive Black B with *Cladosporium cladosporioides* (Dionel *et al*.,

2019), triphenylmethane dye Acid Violet 49 with *Aspergillus fumigatus* (Chaudhry *et al*., 2014), azo dye Reactive Red 2 with *Agaricus bisporus* (Akar and Divriklioglu, 2010), and the azo dye Reactive Blue 4 with *Rhizopus oryzae* (Bagchi *et al*., 2021). RDR2 and RDB4 are anionic dyes, and their binding is favored at low pH because it leads to protonation of the functional groups on the biomass surface, enhancing the electrostatic interactions between the dye molecules and the biomass. Contrarily, an increase in pH results in deprotonation of the functional groups of the biomass surface and an increase in OH- ions, which cause repulsive electrostatic forces between the dye molecules and biomass as well as competition with the OH- ions by the binding sites (Albadarin and Mangwandi, 2015). An increase in the temperature also leads to an increase in the kinetics energy of the dye molecules, improving their intraparticle diffusion rate and, hence, the interactions between dye molecules and binding sites on the biomass surface (Xiong *et al*., 2010). Through these mechanisms, the pH and temperature enhance the biosorption between anionic dyes RDR2 and RDB4 with the *C. tenuissimum* sterilized biomass.

3.3 Effect of contact time and biosorption kinetics evaluation

Contact time is an important factor because it determines the efficiency of the biosorption processes. The biosorbent must be capable of biosorbering rapidly the dye to be a feasible material in the design of biosorption equipment. Figures 5a and 5b show the contact time profiles at 20, 30, and 40ºC for the dyes RDR2 and RDB4. To compare the effect of the temperature at the beginning of the contact time on each of the biosorption kinetics, the initial biosorption rates (dq_t/dt) of each dye were estimated for the temperatures assayed through the slopes of the straight lines fitted by linear regression between the experimental data of q_t and t up to a contact time of 30 min. Initial biosorption rate increase with the temperature of 1.10 mg g^{-1} min^{-1} at 20 ºC to 2.29 mg g^{-1} min^{-1} at 40 ºC for RDR2, and of 0.75 mg g^{-1} min^{-1} at 20 ºC to 1.75 mg g^{-1} min^{-1} at 40 ºC for RDB4. For both dyes and the three temperatures, after 30 min, the biosorption capacity gradually slowed, achieving a faster equilibrium as the temperature increased. This behavior could be attributed to the fact that numerous active sites were initially available for binding, decreasing their availability for biosorption when these functional groups were occupied, reaching saturation more quickly because the diffusion rate of the molecules increased with temperature. The above is indicative that kinetically the biosorption process probably is conducted in an endothermic way.

The biosorption kinetics of RDR2 and RDB4 on sterilized biomass of *C. tenuissimum* were conducted with a dye concentration of 300 mg L^{-1}, pH 5,

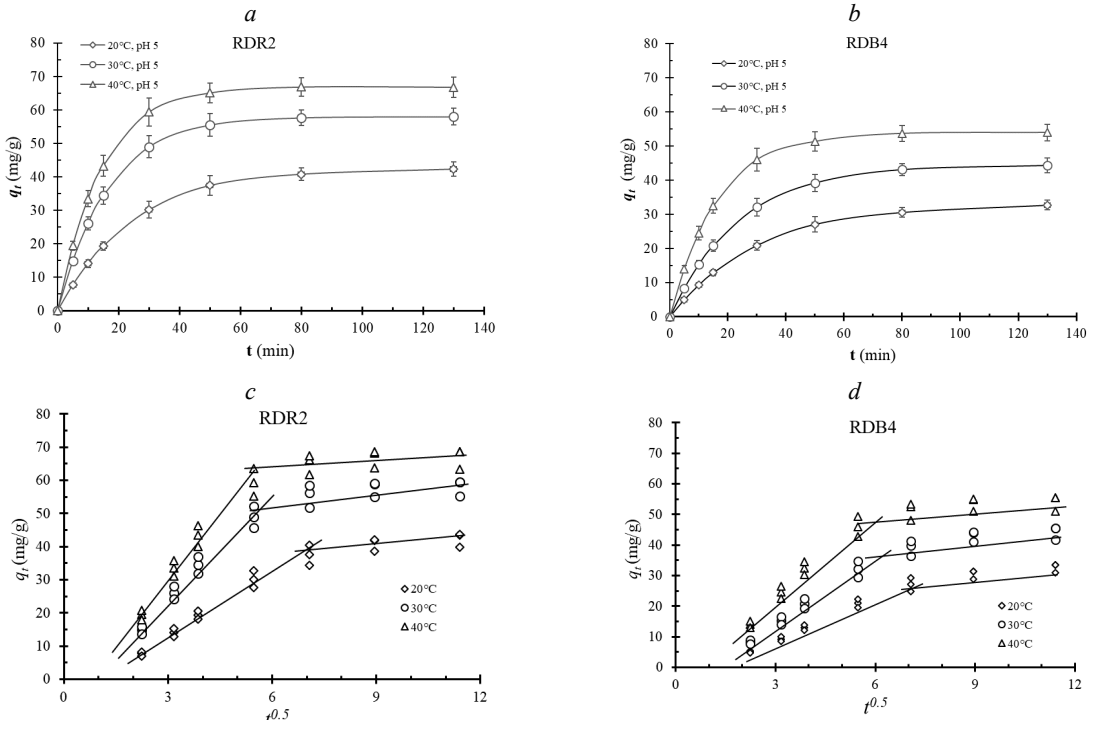

Figure 5. Contact time and kinetic analysis. Effects at pH 5 of the time contact and temperature on the biosorption of the dyes RDR2 (a) and RDB4 (b) onto thermally sterilized biomass of *Cladosporium tenuissimum*. Plots of q_t vs $t^{0.5}$ of the intraparticle model of experimental data for RDR2 (c) and RDB4 (d).

biomass dosage of 5 g L^{-1}, and temperatures of 20, 30, and 40 ºC in times among 5 and 130 min. To evaluate the biosorption process kinetically, kinetic parameters were determined by fitted experimental data to the models pseudo-first-order, pseudo-second-order, and intraparticle diffusion by plotting $\ln(q_e - q_t)$ vs t, t/q_t vs t, and q_t vs $t^{0.5}$, respectively. Table 1 shows the parameter values obtained for each one of the models for RDR2 and RDB4 at the three different temperatures. For both dyes, the model of pseudo-second-order best fits R^2 values between 0.9841 and 0.9917, followed by the diffusion intraparticle model with R^2 values between 0.7488 and 0.9147. In contrast, the pseudo-first-order model has the worst fit with R^2 values between 0.6946 and 0.8720. These results indicate that the biosorption process of RDR2 and RDB4 onto sterilized biomass of *C. tenuissimum* in the three temperatures assayed follows a kinetics of pseudo-second-order. The pseudo-second-order model assumes that the adsorption rate is proportional at the square of the difference between the amount of adsorbate in the adsorbent surface in the time and the maximum amount of adsorbate that can be adsorbed on the surface, and this model has been used to explain chemisorption phenomenon (Lavado-Meza *et al*., 2021). Similar results where the model of pseudo-second-order described kinetically the bisorption of RDR2 and RDB4 onto several biomaterials such as the *Agaricus bisporus* biomass, *Rhizopus oryzae* biomass, chitosan and anaerobic sludge of textile wastewater have been observed (Akar and Divriklioglu, 2010; Bagchi *et al*., 2021; Karmaker *et al*., 2020; Sonai *et al*., 2016).

The Weber and Morris model assumes that diffusion is the limiting mechanism of the adsorption velocity, in which for the graphic of adsorbate adsorbed (q_t) versus the squared root of time ($t^{0.5}$) if the straight line crosses the origin, diffusion is the only mechanism that controls the adsorption. In the fit of the biosorption experimental data of RDR2 and RDB4 to the intraparticle diffusion model, the intersection values to the origin (B) are different from zero, indicating that the diffusion of the dye molecules is not the only limiting mechanism in the biosorption (Figures 5c and 5d). In the biosorption process for both dyes and at the three temperatures, two stages can be observed, which are marked with straight lines. In the first stage, although straight lines are not across the origin, their trend indicates that the diffusion rate is the principal mechanism at the beginning of the biosorption process. It is important to note that at 20 ºC and for both dyes, the straight line is closer to crossing the origin, whereas, for increases in the temperature, the straight lines move away from the origin. The above can be interpreted as a temperature effect where the kinetic energy of the dyes molecules increase with the temperature, which leads to parallel mechanism at the diffusion in than a greater number of interactions of the molecule dyes are given with the functional groups or active sites on the biomass surface. In the second stage, diffusion is less of to be the principal mechanism that controls the biosorption, and the adsorbate-biosorbent interactions dominate the process until biomass surface saturation is reached.

3.4 Isotherms biosorption evaluation of the equilibrium

The equilibrium of RDR2 and RDB4 with the sterilized biomass of *C. tenuissimum* was evaluated through the isotherms models of Langmuir, Temkin, and Dubinin-Radushkevich (D-R). Experimentally, isotherms were constructed by the combination of three different pH (3, 5, 7) with three different temperatures (20, 30, and 40 ºC), determining q_e and C_e to the 10 hours with a biomass dosage of 1-5 g L^{-1} and C_0 of 300 mg L^{-1}. Fitted experimental data allowed determining the parameters of the isotherms by plotting C_e/q_e vs C_e, ln q_e vs ln C_e, and ln q_e vs ε^2 to the models of Langmuir, Temkin, and D-R, respectively. Tables 2 show the biosorption parameters for RDR2 and RDB4, and Figures 6 and 7 show the Langmuir isotherms predicted by the fit to the experimental data. For both dyes, from the figures, it is observed that biosorption capacity improves with a decrease in the pH and an increase in the temperature, having the higher value in the biosorption capacity for a pH of 3 and temperature of 40 ºC. In Tables 2 it also observed that the Isotherms of Langmuir and Temkin had the best fits experimental data with R^2 and RMSE values from 0.990, 1.646, and 0.991, 1.47 for RDR2, and 0.978, 1.63 and 0.985, 2.01 for RDB4, respectively.

Langmuir isotherm assumes a monolayer biosorption on the biosorbent surface, where the parameters of the isotherm $q_{\max}$ and K_L determine the maximum efficiency of biosorption and affinity of the biosorbent by the adsorbate, respectively. In Table 2 for RDR2 and RDB4, it is observed that with a pH decrease from 7 to 3 and temperature increases of 20 to 40 ºC, the values of $q_{\max}$ and K_L increasing for RDR2 from 35.85 to 76.67 mg g^{-1}, and 0.0456 to 0.1259 L mg^{-1}, while for RDB4 increasing from 26.03 to 70.60 mg g^{-1}, and 0.0321 to 0.0882 L mg^{-1}, respectively. The increases in $q_{\max}$ and K_L could be interpreted as an improvement in the interactions between the dye molecules and the active sites or functional groups of the biomass surface. When the pH decreased, and the temperature increased, the number of protonated active sites was greater, and the kinetic energy of the dye molecules increased, favoring the contact and intensity of the interactions between the active sites and the anionic molecules of the dyes RDR2 and RDB4.

Table 1. Kinetic biosorption parameters (biomass dosage 5 g L^{-1} and pH 5) of RDR2 and RDB4 on the thermally sterilized *Cladosporium tenuissimum* biomass at different temperatures.

		Pseudo-first-order model			Pseudo-second-order model			Intraparticle diffusion model		
Dye	T(ºC)	q_e (mg g^{-1})	k_1(min^{-1})	R^2	q_e (mg g^{-1})	k_2(g mg^{-1} min^{-1})	R^2	k_D(mg g^{-1} $min^{-0.5}$)	B (min^{-1})	R^2
RDR2	20	39.63±2.65	0.0148±0.00101	0.8588	51.84±3.35	0.00078±0.00005	0.9861	3.93±0.254	3.79±0.240	0.8776
	30	44.98±2.84	0.0196±0.00128	0.7660	65.14±4.26	0.00118±0.00008	0.9900	4.62±0.303	14.38±0.939	0.7853
	40	48.96±3.16	0.0228±0.00148	0.7139	73.74±4.76	0.00131±0.00008	0.9917	4.97±0.320	20.70±1.341	0.7488
RDB4	20	34.65±2.21	0.0044±0.00028	0.8720	41.89±2.68	0.00072±0.00005	0.9841	3.15±0.202	0.77±0.045	0.9147
	30	43.13±2.73	0.0043±0.00027	0.8103	53.49±3.39	0.00081±0.00005	0.9866	4.05±0.257	4.63±0.295	0.8723
	40	40.79±2.68	0.0044±0.00029	0.6946	60.47±3.98	0.00130±0.00008	0.9897	4.27±0.281	13.69±0.895	0.7820

Table 2. Biosorption parameters at different pH and temperatures of RDR2 and RDB4 on the thermally sterilized *Cladosporium tenuissimum* fungus biomass, determined by fitted to the isotherms of Langmuir, Temkin, and Dubinin-Radushkevich (D-R).

			Langmuir					Temkin				Dubinin-Radushkevich				
Dye	pH	T(ºC)	q_{max} (mg/g)	K_L (L/mg)	R_L	R^2	RMSE	b_T (J/mol)	K_T (L/mg)	R^2	RMSE	q_{DR} (mg/g)	K_{DR} (mol^2/J^2)	E(J/mol)	R^2	RMSE
RDR2	3	20	60.34±3.4	0.0637±0.003	0.0497±0.001	0.957	1.68	307.98±1.5	0.840±0.04	0.973	2.90	42.56±1.0	1.33E-06	627.2±14.2	0.795	11.57
		30	65.73±2.8	0.0874±0.005	0.0369±0.002	0.945	3.32	227.03±4.7	1.541±0.09	0.966	3.43	49.63±0.8	2.72E-06	844.4±14.6	0.882	11.33
		40	76.67±2.3	0.1259±0.001	0.0269±0.001	0.972	4.02	172.79±1.2	1.72±0.04	0.952	5.55	53.97±1.7	3.45E-07	1203.3±24.5	0.770	16.91
	5	20	43.80±2.7	0.0559±0.005	0.0569±0.002	0.974	1.64	280.19±9.2	0.66±0.03	0.984	1.57	37.56±2.3	1.47E-06	587.1±45.8	0.857	9.90
		30	59.48±2.6	0.0749±0.003	0.0426±0.004	0.980	2.78	210.26±7.8	0.90±0.08	0.980	2.62	43.04±1.0	1.02E-06	700.4±17.2	0.775	12.48
		40	68.63±1.7	0.0939±0.003	0.0343±0.001	0.937	2.30	204.75±4.1	1.37±0.03	0.978	3.10	48.46±1.3	5.61E-07	943.9±3.7	0.791	13.62
	7	20	35.85±1.4	0.0456±0.002	0.0682±0.002	0.928	2.94	422.8±10.8	1.06±0.06	0.872	3.06	24.47±0.8	3.03E-06	406.3±6.7	0.931	9.98
		30	51.34±1.9	0.0632±0.016	0.0503±0.004	0.990	1.76	234.9±2.9	0.68±0.02	0.991	1.47	38.12±1.3	1.55E-06	569.7±30.5	0.813	10.48
		40	55.93±2.4	0.0740±0.005	0.0432±0.008	0.946	4.45	201.30±4.0	0.66±0.05	0.985	2.34	42.06±0.8	4.04E-06	685.5±21.9	0.717	13.61
RDB4	3	20	42.81±0.9	0.0500±0.002	0.0623±0.003	0.973	2.55	274.49±7.1	0.54±0.04	0.970	2.12	33.62±5.3	2.94E-06	412.7±11.2	0.864	8.25
		30	52.84±3.2	0.0618±0.003	0.0513±0.003	0.978	2.57	246.3±3.3	0.83±0.06	0.953	3.33	38.41±6.9	1.56E-06	567.7±19.0	0.795	10.06
		40	70.60±3.8	0.0882±0.007	0.0365±0.001	0.893	3.21	215.2±4.5	1.53±0.07	0.965	3.83	51.17±1.5	6.28E-06	892.6±13.4	0.892	12.29
	5	20	33.97±1.7	0.0419±0.003	0.0740±0.005	0.959	2.31	380.4±13.0	0.56±0.05	0.913	2.51	25.69±0.7	4.50E-06	348.9±14.9	0.883	5.92
		30	45.82±1.8	0.0501±0.002	0.0624±0.001	0.977	2.08	287.8±8.5	0.67±0.03	0.957	2.61	33.85±1.1	2.38E-06	458.2±12.0	0.864	8.17
		40	55.40±4.9	0.0687±0.006	0.0465±0.004	0.963	3.49	203.6±4.9	0.63±0.03	0.985	2.29	41.18±0.9	1.22E-06	642.8±30.0	0.732	13.03
	7	20	26.03±1.0	0.0321±0.001	0.0947±0.001	0.955	2.11	449.2±22.2	0.35±0.01	0.903	2.07	19.71±0.6	7.88E-06	258.2±2.2	0.831	9.06
		30	36.64±1.4	0.0397±0.001	0.0775±0.002	0.954	2.13	364.2±8.1	0.55±0.04	0.953	2.01	27.62±0.6	3.95E-06	355.7±6.6	0.916	6.33
		40	44.81±1.9	0.0483±0.004	0.0646±0.002	0.973	1.63	277.8±19.4	0.53±0.03	0.974	2.07	33.46±1.3	2.52E-06	446.2±11.2	0.780	8.55

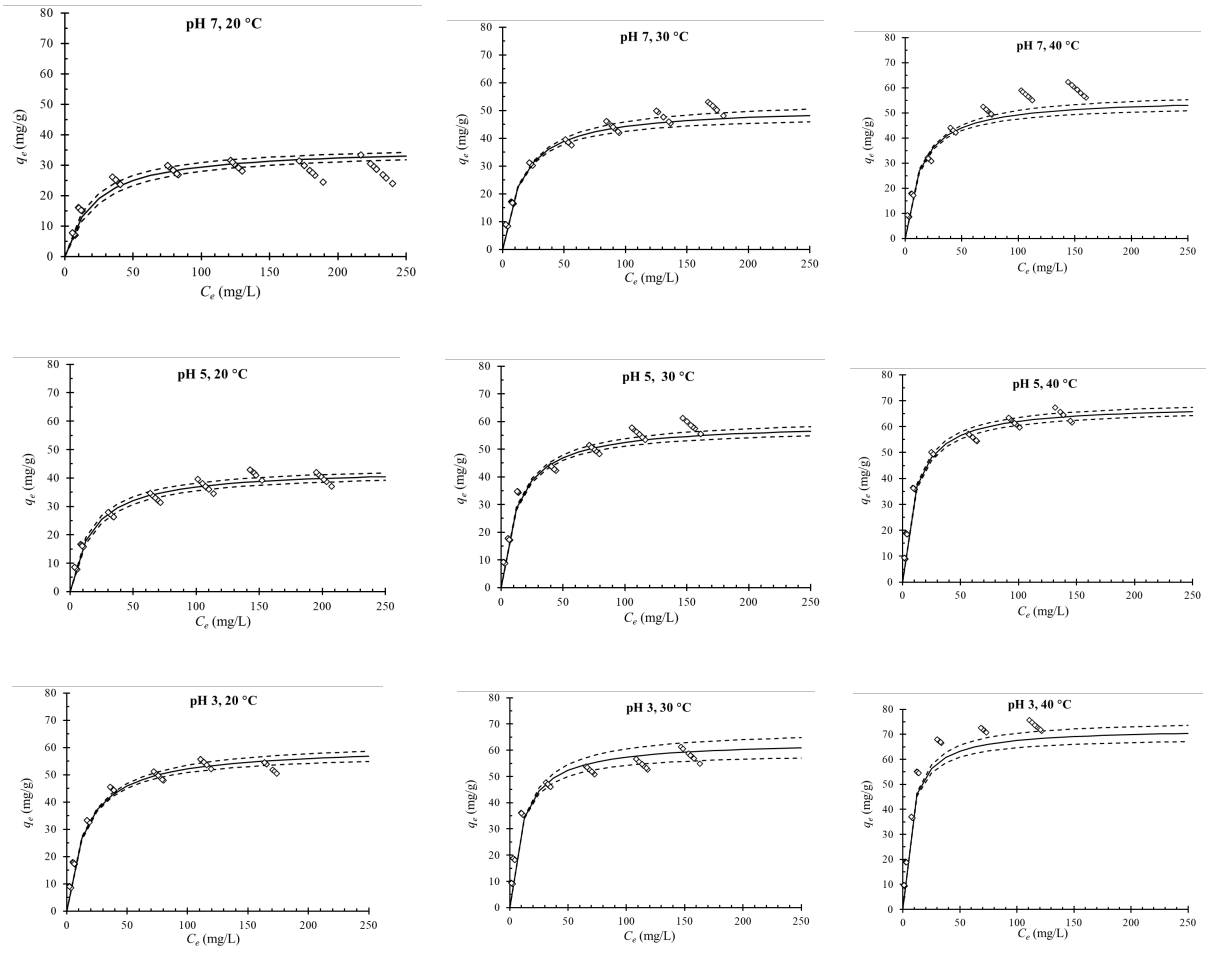

Figure 6. Biosorption isotherms RDR2 on thermally sterilized biomass of *Cladosporium tenuissimum* at different pH (3, 5, 7) and temperatures (20 ºC, 30 ºC, 40 ºC), where ◊ represent the dye sorption experimental data, — the average Langmuir isotherm fitted to experimental data, and - - - the upper and lower values of the isotherm of Langmuir fitted to the experimental data.

The above is also supported for both dyes, with a decreasing trend in the dimensionless separation factor R_L. In all the isotherms, the R_L values remained between 0 and 1, indicating that biosorption of the dyes in fungus biomass, in principle, is favorable and reversible. However, with a pH decrease (7-3) and temperature increase (20-40 ºC), the R_L values tend to decrease from 0.0682 to 0.0260 for RDR2 and from 0.0947 to 0.0365 for RDB4, indicating that in the biosorption process, the equilibrium is displaced preferentially toward the binding of molecule with the biomass surface that in their free form on the solution, which is due to the strengthening of the interactions of the molecules with the active sites.

Temkin isotherm considers that the adsorbent surfaces are heterogeneous, and therefore, there are active sites with different adsorption energies, which is reflected in the KT value, the equilibrium binding energy (L g^{-1}). In Table 2 it is observed that in a similar way to the K_L of Langmuir and for both dyes, when the pH decreases from 7 to 3, and the temperature increases from 20 to 40 ºC, the K_T values increase from 1.06 to 1.72 L mg^{-1} for RDR2, and from 0.35 to 1.53 L mg^{-1} for RDB4, respectively. It is more suitable to assume that biomass surface has a nature heterogeneous (Temkin) than homogeneous (Langmuir). However, both models, Temkin and Langmuir, lead to the same approach, where the biosorption mechanism was enhanced by mean of the protonation of the biosorbent surface via a decrease of the pH and for the increase of intraparticle diffusion rate of the dye molecules via an increase of the temperature. On the other hand, the binding free energy E (kJ mol^{-1}) determined through the Dubinin-Radushkevich isotherm follows the same behavior mentioned above. Nevertheless, the more important to highlight are their magnitude values, since even at pH 3 and temperature of 40 ºC, the values were lesser than 8 kJ mol^{-1} (1.203 and 0.892 kJ mol^{-1}, for RDR2 and RDB4, respectively), indicative that biosorption is type physical and reversible (Saleh, 2022). It is also important to note that when comparing the biosorption capacity between both dyes, the values for RDR2 were greater than RDB4.

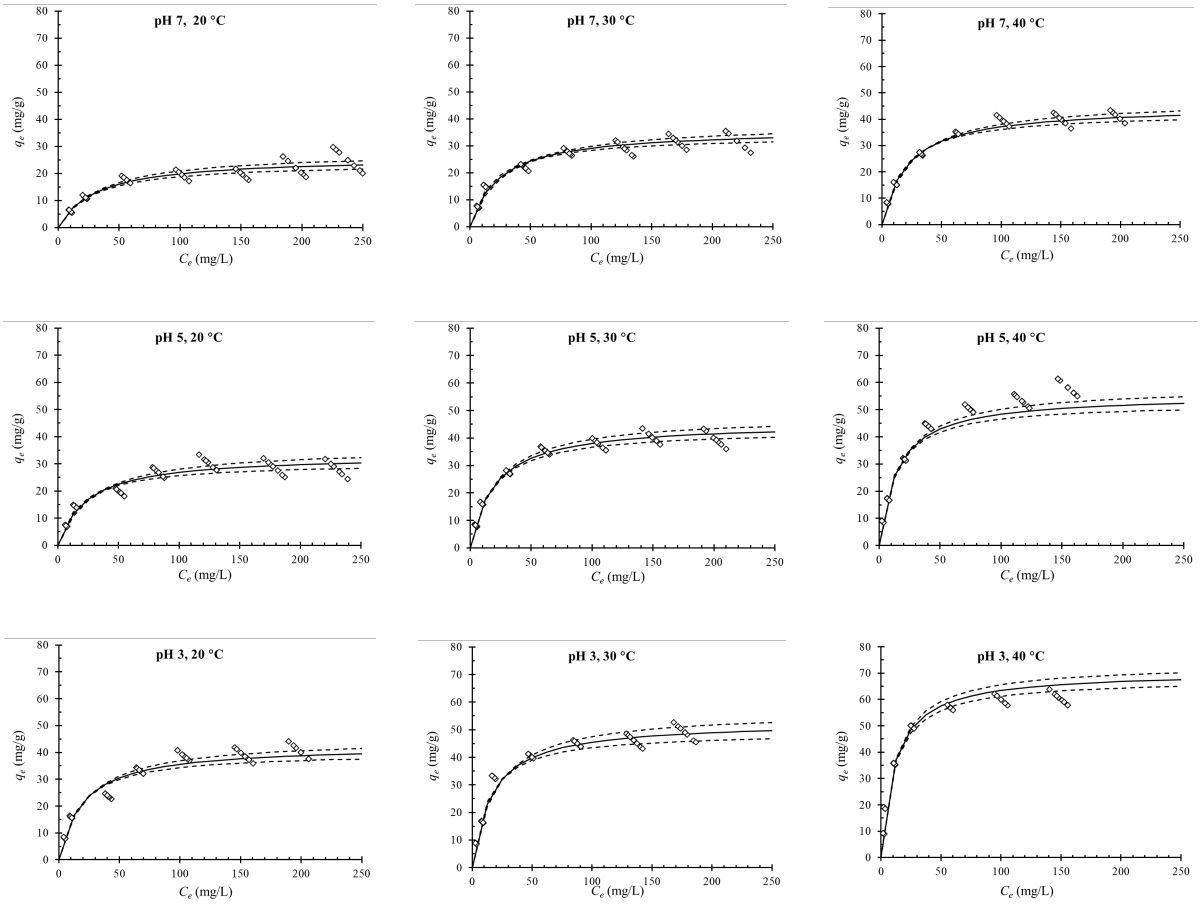

Figure 7. Biosorption isotherms RDB4 on thermally sterilized biomass of *Cladosporium tenuissimum* at different pH (3, 5, 7) and temperatures (20 ºC, 30 ºC, 40 ºC), where ◊ represent the dye sorption experimental data, — the average Langmuir isotherm fitted to experimental data, and - - - the upper and lower values of the isotherm of Langmuir fitted to the experimental data.

Although the number and kinds of interactions could be similar for both dye molecules, the specific surface area available of the biosorbent (fungus biomass) to bind the dye molecules was lesser for RDB4 probably because their molecule size is higher than RDR2.

Table 3 shows a comparison of the maximum biosorption capacity (q_{max}) values reported and determined through the Langmuir isotherm of RDR2 and RDB4 onto different biomaterials, indicating whether the biomaterial was modified previous to the biosorption process as well as pH and temperature of the biosorption assay. The q_{max} values for diverse biomaterials on RDR2 were between 29.76 and 217.70 mg g^{-1}. While for RDB4, the q_{max} values were between 13.20 and 666.70 mg g^{-1}. Biomaterials used as biosorbents include fungal biomass (*Agaricus bisporus*, *Rhizopus oryzae*), bacterial biomass (*Corynebacterium glutamicum*, *Bacillus subtilis*), plants (*Nymphaea rubra*, *Alyssum caricum*), fruit (*Tamarindus indica*), shells (cocoa, chicken egg), chitin, chitosan, sugar cane bagasse, and textile sludge. Compared with other studies, the q_{max} values obtained in the present study on the biosorption of RDR2 and RDB4 onto thermally sterilized biomass of *C. tenuissimum* were placed in an intermediate position (76.67 and 70.60 mg g^{-1}, respectively). It is interesting to observe that the studies that reported the highest q_{max} values were with biomaterials previously modified chemically. In principle, this is beneficial because the biosorption capacity of the materials is improved.

3.5 Bisorption thermodynamic evaluation

To evaluate the thermodynamic of the biosorption of RDR2 and RDB4 onto sterilized biomass of *C. tenuissimum*, the changes of free energy (ΔG), enthalpy (ΔH), and entropy (ΔS) of the process were determined at the three levels of initial pH assayed at the temperatures of 20, 30 and 40 ºC. In Table 4, it is observed for both dyes that the free energy change values for all the pH and temperature levels of biosorption assayed were similar (-24.95 to -29.29 kJ mol^{-1} for RDR2 and -24.18 to -28.46 kJ mol^{-1} for RDB4) and negatives (ΔG<0), which indicates that the

Table 3. Comparative study on the maximum biosorption capacity (q_{max}) of the dyes RDR2 and RDB4 onto different biomaterials.

Dye	Biosorbent (biomaterial)	Biosorption conditions	q_{max} (mg g^{-1})	Reference
RDR2	*Agaricus bisporus* (fungus)	Chemical biomass modification with cetyl trimethyl ammonium bromide, assay pH 2, 45 ºC	141.5	Akar and Divriklioglu (2010)
	Cocoa shell (waste)	Physicochemical biomass modification with non-thermal plasma, assay pH 2, 25 ºC	40.32	Takam *et al*. (2017)
	Tamarindus indica (fruit)	Without biomass modification, assay pH 2, 30 ºC	102.04	Renganathan *et al*. (2008)
	Nymphaea rubra (plant)	Without biomass modification, assay pH 2, 30 ºC	66.67	Renganathan *et al*. (2009)
	Chitin (crab shells)	Without biomass modification, assay pH 3, 45 ºC	29.76	Wu *et al*. (2012)
	Alyssum caricum (plant)	Chemical biomass modification with epichlorohydrin/hexamethylenediamine, assay pH 3, 45 ºC	51.80	Bayramoglu *et al*. (2013)
	Textile sludge	Thermally biomass modification with pyrolysis at 500 ºC, assay pH 2, 45 ºC	217.70	Sonai *et al*. (2016)
	Cladosporium tenuissimum (fungus)	Thermally biomass sterilized (121ºC, 30 min), assay pH 3, 40 ºC	76.67	This study
RDB4	Chitosan 10 B (chitin deacetylated)	Without biomass modification, assay pH 4, 36 ºC	58.57	Karmaker *et al*. (2020)
	Sugar cane bagasse (waste)	Chemical biomass modification with propionic acid, assay pH 2, 27 ºC	13.20	Said *et al*. (2013)
	Rhyzopus oryzae (fungus)	Thermally biomass sterilized (121ºC, 15 min), assay pH 3, 35 ºC	317.25	Bagchi *et al*. (2021)
	Chicken eggshell (waste)	Chemical biomass modification with iron (III) oxide-hydroxide and zinc oxide, assay pH 3, 30 ºC	30.48	Praipipat *et al*. (2022)
	Corynebacterium glutamicum (bacteria)	Chemical biomass modification with HNO_3 1 M 24 h, assay pH 2, room temperature	184.90	Won *et al*. (2008)
	Chitosan	Chemical biomass modification with hexadecylamine and 3-aminopropyl triethoxysilane 24 h, assay pH 4, 30 ºC	666.70	Vakili *et al*. (2017)
	Bacillus subtilis (bacteria)	Thermally biomass sterilized (121ºC, 15 min) and immobilized in sodium alginate beads, assay pH 1, room temperature	42.93	Binupriya *et al*. (2010)
	Chitosan	Chemical biomass modification with hydroxyapatite nanocomposites, assay pH 4, 25 ºC	212.00	Rastgordani *et al*. (2021)
	Cladosporium tenuissimum (fungus)	Thermally biomass sterilized (121ºC, 30 min), assay pH 3, 40 ºC	70.60	This study

process was spontaneous. The enthalpy change values in Table 4 for both dyes show an effect due to pH decreases, where enthalpy increased for RDR2 from 18.52 to 25.94 kJ mol^{-1} when pH variation is from 7 to 3. While for RDB4, the enthalpy change increased from 15.58 to 21.57 kJ mol^{-1} in the same decrease of the pH. The magnitude of the enthalpy change allows it to infer the kind of interaction that occurs (Lavado-Meza *et al*., 2021). Values of ΔH<30kJ mol^{-1}, indicate physical adsorption, where ranges of 4 to 10 kJ mol^{-1} and 2 to 29 kJ mol^{-1} are associated with forces of van der Waals and dipole-dipole bonds, respectively. The positive values of the enthalpy change with the temperature increase indicate that the biosorption process for both dyes was endothermic, behavior also reported in the biosorption of others dyes on fungal biomass (Akar and Divriklioglu, 2010; Xiong *et al*., 2010; Chaudhry *et al*., 2014; Grassi

Table 4. Thermodynamic biosorption parameters at different pH and temperatures of RDR2 and RDB4 on the thermally sterilized *Cladosporium tenuissimum* biomass.

		pH 3			pH 5			pH 7		
Dye	T(ºC)	ΔG^o (kJ/mol)	ΔH^o (kJ/mol)	ΔS^o (kJ/mol K)	ΔG^o (kJ/mol)	ΔH^o (kJ/mol)	ΔS^o (kJ/mol K)	ΔG^o (kJ/mol)	ΔH^o (kJ/mol)	ΔS^o (kJ/mol K)
RDR2	20	-25.76	25.94	0.1764	-25.45	19.79	0.1545	-24.95	18.52	0.1486
	30	-27.43			-27.05			-26.62		
	40	-29.29			-28.53			-27.91		
RDB4	20	-25.26	21.57	0.1596	-24.83	18.79	0.1487	-24.18	15.58	0.1357
	30	-26.66			-26.13			-25.54		
	40	-28.46			-27.81			-26.89		

et al., 2019). The temperature increases give the energy to overcome the repulsion between the dye molecules and the biomass surface. According to the magnitude of the values, the biosorption must be physical with interactions of type dipole-dipole between molecules of dyes and biomass surface. As was discussed above, the force of the interactions between dye molecules and active sites of the biomass is enhanced by the protonation of the biomass surface by the pH decreased. The low positive values in the entropy change (ΔS ≤0.1764 kJ mol^{-1} K^{-1} for RDR2 and ΔS ≤0.1596 kJ mol^{-1} K^{-1} for RDB4) indicate a minimum disorder or randomness in the biosorption process, probably due to a high and specific interaction between dye molecules and the functional groups of the active sites on the biomass surface.

3.6 FTIR analysis

In order to identify the main functional groups involved in the biosorption of RDR2 and RDB4 onto sterilized biomass of *C. tenuissimum*, FTIR analysis between 4000 and 500 cm^{-1} of the biomass thermally inactive unloaded and loaded with each one of the dyes was conducted. Figure 8a shows the frequency of the peaks identified in the inactive biomass unloaded. A broad band around the peak at 3287 cm^{-1} can correspond to the -NH_2 asymmetric stretch of amines and bonded -OH groups (Chaudhry *et al*., 2014). The 2923 and 2858 cm^{-1} peaks represent the -CH symmetric stretching associated with the fatty acids (Bagchi *et al*., 2021). The peak at 1728 cm^{-1} can be assigned to C=O (Akar and Divriklioglu, 2010), while the peaks at 1657, 1562, and 1371 cm^{-1} are within ranges that correspond to amides groups I, II, and III, respectively (Chaudhry *et al*., 2014). The last three peaks at 1075, 1025, and 583 cm^{-1} are associated with -P-OH (Bayramoglu *et al*., 2013), -C-O (Akar and Divriklioglu, 2010), and -C-N-C-, which is characteristic of the structure protein (Diniz *et al*., 2016).

FTIR spectrums of biomass unloaded and loaded with RDR2 are displayed in Figure 8b. In the wavelength range of 3500-3000 cm^{-1} can be observed for loaded biomass a significative increase of

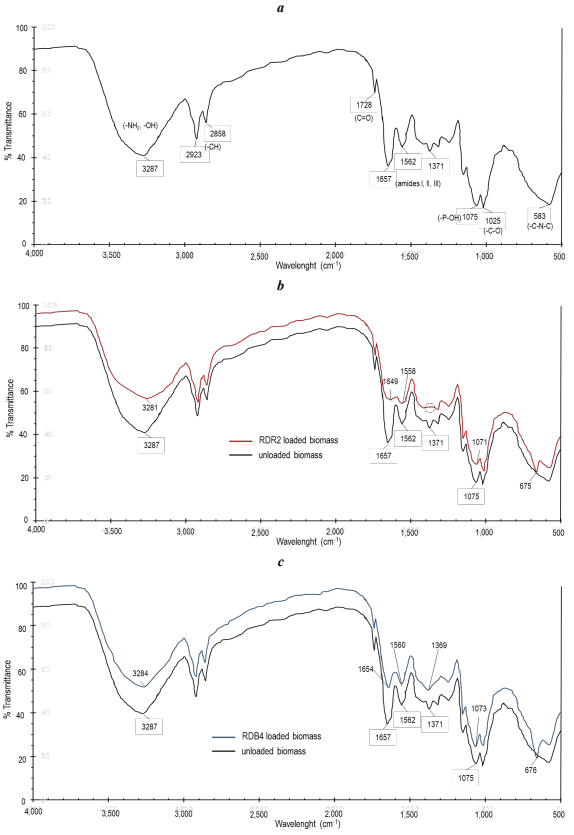

Figure 8. FTIR analysis of the biomass unloaded and loaded with the dyes. (a) FTIR spectrum of unloaded thermally sterilized biomass of *Cladosporium tenuissimum*, (b) FTIR spectrum of unloaded biomass and loaded with RDR2, (c) FTIR spectrum of unloaded biomass and loaded with RDB4.

transmittance percentage, and the peak has been shifted of 3287 at 3281 cm^{-1}, which indicates the binding of RDR2 was probably through their groups sulphonate -SO_3- and chlorine Cl with the -NH_2 amines of the biomass. In the range of 1680-1300 cm^{-1}, there is also an increase in the transmittance percentage with a decrease and shift of the peaks corresponding to amides I and II of 1657 and 1562 cm^{-1} to 1649 and 1558 cm^{-1}, respectively. Moreover, the peak of the amide III is not detected (indicated by a circle with a dashed line). The above is also due to interactions of the RDR2 molecules with the amides

of the biomass. Similarly, for the -P-OH, it is observed that their peak is shifted from 1075 to 1071 cm^{-1}. In the spectrum of the biomass loaded with RDR2, a new peak appears at 675 cm^{-1}, which can be assigned to aromatic -CH symmetric bending vibrations indicating the dye biosorption (Akar *et al*., 2009b).

FTIR spectrums of biomass unloaded and loaded with RDB4 are displayed in Figure 8c. It can be observed similitudes with respect to the biosorption spectrum of RDR2. However, in 3500-3000 cm^{-1}, the peak is greater, indicating a lower increase in the transmittance percentage. Besides, the peak was shifted from 3287 to 3284 cm^{-1}. The peak of the amide III group appears in the range of 1680-1300 cm^{-1}, and for the amides I and II groups, the peaks are a little greater with respect to RDR2 spectrum. The amides group I, II, and III peaks shifted from 1657, 1562, and 1371 cm^{-1} to 1654, 1570, and 1369 cm^{-1}, respectively. In the spectrum of the biomass loaded with RDB4 also appears a new peak but slightly higher at 676 cm^{-1}, which again indicates the dye biosorption for interaction with the aromatic -CH symmetric bending. The shift in the peaks and their different intensities indicate that the RDR2 and RDB4 molecules interacted with the biomass's functional groups during the biosorption process.

Conclusions

The present study showed that the thermally sterilized biomass of the fungus *Cladosporium tenuissimum* has the capacity to remove by biosorption the azo dyes reactive red 2 (RDR2) and reactive blue 4 (RDB4) from aqueous solution. A decrease in the initial pH and an increase in the temperature improved the biosorption of the dyes, with the higher removal efficiencies at pH 3 and a temperature of 40 °C. The biosorption kinetics of both dyes was well explained by a pseudo-second-order model, reaching equilibrium as fast as possible at 50 min and 40 °C. Moreover, the intraparticle diffusion model showed two control stages in the biosorption process, the first by the diffusion rate and the second by the surface saturation with the dye molecules. The Langmuir isotherm explained well the biosorption equilibrium, reached at pH 3 and 40 ºC the maximum biomass biosorption capacities (q_{max}) with values of 76.67 mg g^{-1} for RDR2 and 70.60 mg g^{-1} for RDB4. Furthermore, according to the dimensionless separation factor (R_L) values and the thermodynamic evaluation, the biosorption process is favorable, reversible, spontaneous, and endothermic. FTIR analysis of unloaded and loaded biomass confirmed the interactions between dye molecules and functional groups on the fungal biomass. All the above findings lead to considering the application of the thermally sterilized biomass of *Cladosporium tenuissimum* as a biosorbent biomaterial for bioprocess design in removing the dyes reactive red 2 and reactive blue 4 from textile wastewater. Nevertheless, for possible industrial or technological applications of fungal biomass in the treatment of textile wastewater, it is necessary to evaluate the operational, environmental, and economic feasibility associated with fungal biomass production and pretreatment, as well as biosorption equipment design at laboratory and pilot levels for the scale-up of the process.

References

Abdel-Aty, A.M., Gad-Allah, T.A., Ali, M. E. and Abdel-Ghafar, H.H. (2015). Parametric, equilibrium, and kinetic studies on biosorption of diuron by *Anabaena sphaerica* and *Scenedesmus obliquus. Environmental Progress and Sustainable Energy 34*, 504-511. https://doi.org/10.1002/ep.12027

Ahluwalia, S. S. and Goyal, D. (2010). Removal of Cr (VI) from aqueous solution by fungal biomass. *Engineering in Life Sciences 10*, 480-485. https://doi.org/10.1002/elsc.200900111

Akar, S. T., Gorgulu, A., Kaynak, Z., Anilan, B. and Akar, T. (2009a). Biosorption of Reactive Blue 49 dye under batch and continuous mode using a mixed biosorbent of macro-*fungus Agaricus bisporus* and *Thuja orientalis* cones. *Chemical Engineering Journal 148*, 26-34. https://doi.org/10.1016/j.cej.2008.07.027

Akar, T. and Divriklioglu, M. (2010). Biosorption applications of modified fungal biomass for decolorization of Reactive Red 2 contaminated solutions: Batch and dynamic flow mode studies. *Bioresource Technology 101*, 7271-7277. https://doi.org/10.1016/j.biortech.2010.04.044

Akar, T., Tosun, I., Kaynak, Z., Kavas, E., Incirkus, G. and Akar, S. T. (2009b). Assessment of the biosorption characteristics of a macro-fungus for the decolorization of Acid Red 44 (AR44) dye. *Journal of Hazardous Materials 171*, 865-871. https://doi.org/10.1016/j.jhazmat.2009.06.085

Aksu, Z. and Karabayır, G. (2008). Comparison of biosorption properties of different kinds of fungi for the removal of Gryfalan Black R_L metal-complex dye. *Bioresource Technology 99*, 7730-7741. https://doi.org/10.1016/j.biortech.2008.01.056

Al-Amrani, W. A., Lim, P. E., Seng, C. E. and Ngah, W. S. W. (2014). Factors affecting bio-decolorization of azo dyes and COD removal in anoxic-aerobic REACT operated sequencing batch reactor. *Journal of the Taiwan Institute of Chemical Engineers 45*, 609-616. https://doi.org/10.1016/j.jtice.2013.06.032

Albadarin, A. B. and Mangwandi, C. (2015). Mechanisms of Alizarin Red S and Methylene blue biosorption onto olive stone by-product: Isotherm study in single and binary systems. *Journal of Environmental Management 164*, 86-93. https://doi.org/10.1016/j.jenvman.2015.08.040

Arslan, S., Eyvaz, M., Gürbulak, E. and Yüksel, E. (2016). A review of state-of-the-art technologies in dye-containing wastewater treatment-the textile industry case. *Textile Wastewater Treatment*, 1-29. http://dx.doi.org/10.5772/64140

Axelsson J., Nilsson U., Terrazas E., Aliaga T. Alvarez. and Welander U. (2006). Decolorization of the textile dyes Reactive Red 2 and Reactive Blue 4 using *Bjerkandera sp*. Strain BOL 13 in a continuous rotating biological contactor reactor. *Enzyme and Microbial Technology 39*, 32-37. https://doi.org/10.1016/j.enzmictec.2005.09.006

Azin, E. and Moghimi, H. (2018). Efficient mycosorption of anionic azo dyes by *Mucor circinelloides*: Surface functional groups and removal mechanism study. *Journal of Environmental Chemical Engineering 6*, 4114-4123. https://doi.org/10.1016/j.jece.2018.06.002

Bagchi, M., Bera, D. and Adhikari, S. (2021). Biosorption of an azo dye Reactive Blue 4 from aqueous solution using dead and CMC immobilized biomass of *Rhizopus oryzae* (MTCC 262). *Bioremediation Journal 25*, 326-346. https://doi.org/10.1080/10889868.2021.1884526

Bayramoglu, G., Adiguzel, N., Ersoy, G., Yilmaz, M. and Yakup-Arica, M. (2013). Removal of textile dyes from aqueous solution using amine-modified plant biomass of *A. caricum*: equilibrium and kinetic studies. *Water, Air, & Soil Pollution 224*, 1-16. https://doi.org/10.1007/s11270-013-1640-z

Binupriya, A. R., Sathishkumar, M., Ku, C. S. and Yun, S. I. (2010). Sequestration of reactive blue 4 by free and immobilized *Bacillus subtilis* cells and its extracellular polysaccharides. *Colloids and Surfaces B: Biointerfaces 76*, 179-185. https://doi.org/10.1016/j.colsurfb.2009.10.031

Chaudhry, M. T., Zohaib, M., Rauf, N., Tahir, S. S. and Parvez, S. (2014). Biosorption characteristics of *Aspergillus fumigatus* for the decolorization of triphenylmethane dye acid violet 49. *Applied Microbiology and Biotechnology 98*, 3133-3141. https://doi.org/10.1007/s00253-013-5306-y

Danouche, M., El Arroussi, H., Bahafid, W. and El Ghachtouli, N. (2021). An overview of the biosorption mechanism for the bioremediation of synthetic dyes using yeast cells. *Environmental Technology Reviews 10*, 58-76. https://doi.org/10.1080/21622515.2020.1869839

Dave, D. and Dikshit, A. K. (2014). Efficacy of various biosorbents for removal of endosulfan from water environment. *International Journal of Environmental Engineering 6*, 287-302. https://doi.org/10.1504/IJEE.2014.064304

Dávila-Parra, F. A., Plasencia-Jatomea, M., Monge-Amaya, O., Mártin-García, A. R., De La Vega-Olivas, J. and Almendariz-Tapia, F. J. (2022). Influence of initial copper concentration, pH, and cross-linked alginate-chitosan and alginate-chitosan-*Aspergillus australensis* composite beads on the adsorption capacity and removal efficiency of copper ions. *Revista Mexicana de Ingeniería Química 21*, IA2892. https://doi.org/10.24275/rmiq/IA2892

Diniz, G., Garcia, E. and Cury, J. (2016). Removal of textile dye Novacron Yellow using the fungal biomass based on *Cladosporium sp*. genus. *Scientific Electronic Archives 9*, 118-125. https://doi.org/10.36560/942016335

Dionel, L. A. S., Santos, B. A. P., Lopes, V. C. P., Vasconcelos, L. G., Soares, M. A. and Morais, E. B. (2019). Biosorption of azo dye reactive black B onto nonviable biomass of *Cladosporium cladosporioides* LM1: Thermodynamic, kinetic and equilibrium modeling. *International Journal of Biotechnology and Bioengineering 13*, 78-84. https://doi.org/10.5281/zenodo.2643850

Drummond, A.J., Nicholls, G.K., Rodrigo, A.G. and Solomon, W. (2002). Estimating mutation parameters, population history and genealogy simultaneously from temporally spaced

sequence data. *Genetics 161*, 1307-1320. https://doi.org/10.1093/genetics/161.3.1307

Garza-González, M. T., Ramírez-Vázquez, J. E., García-Hernández, M. D. L. Á., Cantú-Cárdenas, M. E., Liñan-Montes, A. and Villarreal-Chiu, J. F. (2017). Reduction of chromium (VI) from aqueous solution by biomass of *Cladosporium cladosporioides*. *Water Science and Technology 76*, 2494-2502. https://doi.org/10.2166/wst.2017.427

Gonzales-Condori, E.G., Avalos-López, G., Gonzales-Condori, J., Mujica-Guzmán, A., Terán-Hilares, R., Briceño, G., Quispe-Avilés, J.M., Parra-Ocampo, P.J. and Villanueva-Salas, J.A. (2023). Avocado seed powder residues as a promising bio-adsorbent for color removal from textile wastewater. *Revista Mexicana de Ingeniería Química 22*, IA2370. https://doi.org/10.24275/rmiq/IA2370

Grassi, P., Reis, C., Drumm, F. C., Georgin, J., Tonato, D., Escudero, L. B., Kuhn, R., Jahn, S. L. and Dotto, G. L. (2019). Biosorption of crystal violet dye using inactive biomass of the fungus *Diaporthe schini*. *Water Science and Technology 79*, 709-717. https://doi.org/10.2166/wst.2019.091

He, S., Sun, W., Wang, J., Chen, L., Zhang, Y. and Yu, J. (2016). Enhancement of biodegradability of real textile and dyeing wastewater by electron beam irradiation. *Radiation Physics and Chemistry 124*, 203-207. https://doi.org/10.1016/j.radphyschem.2015.11.033

Ho, Y.S. and McKay, G. (1998). Kinetic models for the sorption of dye from aqueous solution by wood. *Process Safety and Environmental Protection 76*, 183-191. https://doi.org/10.1205/095758298529326

Juhasz, A. L., Smith, E., Smith, J. and Naidu, R. (2002). Biosorption of organochlorine pesticides using fungal biomass. *Journal of Industrial Microbiology and Biotechnology 29*, 163-169. https://doi.org/10.1038/sj.jim.7000280

Juhasz, A. L., Smith, E., Smith, J. and Naidu, R. (2003). In situ remediation of DDT-contaminated soil using a two-phase cosolvent flushing-fungal biosorption process. *Water, Air, and Soil Pollution 147*, 263-274. https://doi.org/10.1038/sj.jim.7000280

Karmaker, S., Nag, A. J. and Saha, T. K. (2020). Adsorption of reactive blue 4 dye onto Chitosan 10B in aqueous solution: Kinetic modeling and isotherm analysis. *Russian Journal of Physical Chemistry A 94*, 2349-2359. https://doi.org/10.1134/S0036024420110126

Kumar, K., Singh, G. K., Dastidar, M. G. and Sreekrishnan, T. R. (2014). Effect of mixed liquor volatile suspended solids (MLVSS) and hydraulicretention time (HRT) on the performance of activated sludge process during the biotreatment of real textile wastewater. *Water Resources and Industry 5*, 1-8. https://doi.org/10.1016/j.wri.2014.01.001

Lagergren, S. (1898). Zur theorie der sogenannten adsorption gelöster stoffe Kungliga Svenska Vetenskapsakademiens. *Handlingar 24*, 1-39. https://doi.org/10.1007/BF01501332

Lavado-Meza, C., Asencios, Y. J. O., Cisneros-Santos, G. and Unchupaico-Payano, I. (2021). Removal of methylene blue dye using *Nostoc commune* biomass: kinetic, equilibrium and thermodynamic study. *Revista Mexicana de Ingeniería Química 20*, 941-954. https://doi.org/10.24275/rmiq/IA2291

Legorreta-Castañeda, A. J., Lucho-Constantino, C. A., Coronel-Olivares, C., Beltrán-Hernández, R. I. and Vázquez-Rodríguez, G. A. (2022). Biosorption of precious metals present at dilute concentrations on fungal pellets. *Processes 10*, 645. https://doi.org/10.3390/pr10040645

Liao, C.S., Hung, C.H. and Chao, S.L. (2013). Decolorization of azo dye reactive black B by *Bacillus cereus* strain HJ-1. *Chemosphere 90*, 2109- 2114. https://doi.org/10.1016/j.chemosphere.2012.10.077

Liu, Y. (2009). Is the free energy change of adsorption correctly calculated? *Journal of Chemical and Engineering Data 54*, 1981-1985. https://doi.org/10.1021/je800661q

Medina-Moreno, S.A., Pérez-Cadena, R., Jiménez-González, A., Téllez-Jurado, A. and Lucho-Constantino, C.A. (2012). Modeling wastewater biodecolorization with reactive blue 4 in fixed bed bioreactor by *Trametes subectypus*: Biokinetic, biosorption and transport. *Bioresource Technology 123*, 452-462. https://doi.org/10.1016/j.biortech.2012.06.097

Mustafa, M. M., Jamal, P., Mahmod, S. S., Jimat, D. N. and Ilyas, N. N. (2017). *Panus tigrinus* as a potential biomass source for Reactive Blue decolorization: Isotherm and kinetic

study. *Electronic Journal of Biotechnology 26*, 7-11. https://doi.org/10.1016/j.ejbt.2016.12.001

Nouri, H., Azin, E., Kamyabi, A. and Moghimi, H. (2021). Biosorption performance and cell surface properties of a fungal-based sorbent in azo dye removal coupled with textile wastewater. *International Journal of Environmental Science and Technology 18*, 2545-2558. https://doi.org/10.1007/s13762-020-03011-5 Praipipat, P., Ngamsurach, P., Saekrathok, C. and Phomtai, S. (2022). Chicken and duck eggshell beads modified with iron (III) oxide-hydroxide and zinc oxide for reactive blue 4 dye removal. *Arabian Journal of Chemistry 15*, 104291. https://doi.org/10.1016/j.arabjc.2022.104291

Rangabhashiyam, S., Sujata, L. and Balasubramanian, P. (2018). Biosorption characteristics of methylene blue and malachite green from simulated wastewater onto *Carica papaya* wood biosorbent. *Surfaces and Interfaces 10*, 197-215. https://doi.org/10.1016/j.surfin.2017.09.011

Rastgordani, M. and Zolgharnein, J. (2021). Simultaneous determination and optimization of titan yellow and reactive blue 4 dyes removal using chitosan@ hydroxyapatite nanocomposites. *Journal of Polymers and the Environment 29*, 1789-1807. https://doi.org/10.1007/s10924-020-01982-7

Renganathan, S., Kalpana, J., Dharmendira Kumar, M. and Velan, M. (2009). Equilibrium and kinetic studies on the removal of Reactive Red 2 dye from an aqueous solution using a positively charged functional group of the *Nymphaea rubra* biosorbent. *CLEAN-Soil, Air, Water 37*, 901-907. https://doi.org/10.1002/clen.200900133

Renganathan, S., Seenuvasan, M., Selvaraj, S., Gautam, P. and Velan, M. (2008). Equilibrium and kinetic modeling on biosorption of reactive red 2 using *Tamarindus indica* fruit hulls. *Chemical Product and Process Modeling 3*. https://doi.org/10.2202/1934-2659.1143

Robles-Morales, D. L., Reyes Cervantes, A., Díaz-Godínez, R., Tovar-Jiménez, X., Medina-Moreno, S. A. and Jiménez-González, A. (2021). Design and performance evaluation of a fungi-bacteria consortium to biodegrade organic matter at high concentration on synthetic slaughterhouse wastewater. *Water, Air, and Soil Pollution 232*, 223. https://doi.org/10.1007/s11270-021-05177-1

Said, A. E. A. A., Aly, A. A., Abd El-Wahab, M. M., Soliman, S. A., Abd El-Hafez, A. A., Helmey, V. and Goda, M. N. (2013). Application of modified bagasse as a biosorbent for reactive dyes removal from industrial wastewater. *Journal of Water Resource and Protection 5*, 10. http://dx.doi.org/10.4236/jwarp.2013.57A003

Saleh, T. A. (2022). Isotherm models of adsorption processes on adsorbents and nanoadsorbents. *Interface Science and Technology 34*, 99-126. https://doi.org/10.1016/B978-0-12-849876-7.00009-9 Saratale, R. G., Saratale, G. D., Chang, J. S. and Govindwar, S. P. (2011). Bacterial decolorization and degradation of azo dyes: a review. *Journal of the Taiwan institute of Chemical Engineers 42*, 138-157. https://doi.org/10.1016/j.jtice.2010.06.006

Singh, S. and Khajuria, R. (2018). *Penicillium* enzymes for the textile industry. *New and Future Developments in Microbial Biotechnology and Bioengineering*, 201-215. https://doi.org/10.1016/B978-0-444-63501-3.00011-9

Sonai, G. G., de Souza, S. M. G. U., de Oliveira, D. and de Souza, A. A. U. (2016). The application of textile sludge adsorbents for the removal of Reactive Red 2 dye. *Journal of Environmental Management 168*, 149-156. https://doi.org/10.1016/j.jenvman.2015.12.003

Takam, B., Acayanka, E., Kamgang, G. Y., Pedekwang, M. T. and Laminsi, S. (2017). Enhancement of sorption capacity of cocoa shell biomass modified with non-thermal plasma for removal of both cationic and anionic dyes from aqueous solution. *Environmental Science and Pollution Research 24*, 16958-16970. https://doi.org/10.1007/s11356-017-9328-3

Thompson, J.D., Gibson, T.J., Plewniak, F., Jeanmougin, F. and Higgins, D.G. (1997). The CLUSTAL X Windows interface: flexible strategies for multiple sequence alignment aided by quality analysis tools. *Nucleic Acids Research 24*, 4876-4882. https://doi.org/10.1093/nar/25.24.4876 Vakili, M., Rafatullah, M., Ibrahim, M. H., Abdullah, A. Z., Gholami, Z. and Salamatinia, B. (2017). Enhancing reactive blue 4 adsorption through chemical modification of chitosan with hexadecylamine and 3-aminopropyl triethoxysilane. *Journal of Water Process Engineering 15*, 49-54. https://doi.org/10.1016/j.jwpe.2016.06.005

Weber Jr, W. J. and Morris, J. C. (1963). Kinetics of adsorption on carbon from solution. *Journal of the Sanitary Engineering Division 89*, 31-59. https://doi.org/10.1061/JSEDAI.0000430

Whelan, S. and Goldman, N. (2001). A general empirical model of protein evolution derived from multiple protein families using a maximum-likelihood approach. *Molecular Biology and Evolution 18*, 691-699. https://doi.org/10.1093/oxfordjournals.molbev.a003851

Won, S. W., Han, M. H. and Yun, Y. S. (2008). Different binding mechanisms in biosorption of reactive dyes according to their reactivity. *Water Research 42*, 4847-4855. https://doi.org/10.1016/j.watres.2008.09.003

Wu, C. H., Kuo, C. Y., Yeh, C. H. and Chen, M. J. (2012). Removal of CI Reactive Red 2 from aqueous solutions by chitin: An insight into kinetics, equilibrium, and thermodynamics. *Water Science and Technology 65*, 490-495. https://doi.org/10.2166/wst.2012.878

Xiong, X. J., Meng, X. J. and Zheng, T. L. (2010). Biosorption of CI Direct Blue 199 from aqueous solution by nonviable *Aspergillus niger. Journal of Hazardous Materials 175*, 241-246. https://doi.org/10.1016/j.jhazmat.2009.09.155